Carboxyl-Terminal Disulfide Bond of Acid Sphingomyelinase Is Critical for Its Secretion and Enzymatic Function†

Ching Yin Lee,‡ Taku Tamura,§ Nadia Rabah,|| Dong-Young Donna Lee,‡ Isabelle Ruel,‡ Anouar Hafiane,‡ Iulia Iatan,‡ Dana Nyholt,‡ Frédéric Laporte,⊥ Claude Lazure,|| Ikuo Wada,§ Larbi Krimbou,‡ and Jacques Genest*,‡

Cardiovascular Genetics Laboratory, Cardiology Division, McGill University Health Center/Royal Victoria Hospital, Montréal, Québec H3A 1A1, Canada, Department of Cell Science, Institute of Biomedical Sciences, Fukushima Medical University School of Medicine, Fukushima, Japan, Laboratory of Structure and Metabolism of Neuropeptides, Institut de recherches cliniques de Montreal, Montréal, Canada, and Cell Map Laboratory, McGill University, Montréal, Canada

Received April 30, 2007; Revised Manuscript Received October 26, 2007

ABSTRACT: The human acid sphingomyelinase (ASM, EC 3.1.4.12), a lysosomal and secretory protein coded by the sphingomyelin phosphodiesterase 1 (SMPD-1) gene, catalyzes the degradation of sphingomyelin (SM) to ceramide and phosphorylcholine. We examined the structural−functional properties of its carboxyl-terminus (amino acids 462−629), which harbors ~1/3 of all mutations discovered in the SMPD-1 gene. We created four naturally occurring mutants (ΔR608, R496L, G577A, and Y537H) and five serial carboxyl-terminal deletion mutants (N620, N590, N570, N510, and N490). Transient transfection of the His/V5-tagged wild-type and mutant recombinant ASM in Chinese hamster ovary cells showed that all the mutants were normally expressed. Nonetheless, none of them, except the smallest deletion mutant N620 that preserved all post-translational modifications, were found capable of secretion to the medium. Furthermore, only the N620 conserved functional integrity (100% activity of the wild type); all other mutants completely lost the ability to catalyze SM hydrolysis. Importantly, cell surface biotinylation revealed that mutant ΔR608 transfected CHO cells and fibroblasts from a compound heterozygous Niemann−Pick disease type B (NPD-B) patient (ΔR608 and R441X) have defective translocation to the plasma membrane. Furthermore, we demonstrated that the ΔR608 and N590 were trapped in the endoplasmic reticulum (ER) quality control checkpoint in contrast to the wild-type lysosomal localization. Interestingly, while the steady-state levels of ubiquitination were minimal for the wild-type ASM, a significant amount of Lys63-linked polyubiquitinated ΔR608 and N590 could be purified by S5a-affinity chromatography, indicating an important misfolding in the carboxyl-terminal mutants. Altogether, we provide evidence that the carboxyl-terminus of the ASM is crucial for its protein structure, which in turns dictates the enzymatic function and secretion.

Sphingomyelinase (sphingomyelin phosphodiesterase) hydrolyzes sphingomyelin (SM)[1] to form phosphocholine and ceramide (*1*). Several enzymes catalyzing this reaction have been described (*2*). The acidic form of sphingomyelinase, ASM (EC 3.4.12), is a product of the sphingomyelin phosphodiesterase 1 (SMPD-1) gene. It works at optimal pH of 5.0 and is ubiquitiously distributed in all mammalian tissues (*3*). Schissel et al. (*4*) have shown that the same gene gives rise to two different products, lysosomal ASM and secretory ASM, presumably by differential posttranslational modification.

Deficiency of the ASM enzyme due to mutations in SMPD-1 leads to the inherited sphingolipidosis Niemann−Pick disease types A and B (*5*). In the study of this metabolic defect, ASM has been shown to be implicated in many important physiological and pathological processes involving SM hydrolysis. For example, ASM plays an important role in the regulation of the metabolism of biologically active sphingolipids, including ceramide and sphingosine 1-phosphate, which in turn are key players in cancer pathogenesis (*6, 7*), cellular differentiation, and various immune and inflammatory responses (*8, 9*). Our laboratory and others have also demonstrated that ASM is involved in the regulation of intracellular cholesterol trafficking and metabolism (*10*). Because SM and cholesterol are membrane lipids with important structural roles in the regulation of the fluidity and subdomain structure of the lipid bilayers (*11*), it is conceivable that any elevation of SM and secondary

† This research was supported in part by Grants CIHR MOP 15042 and CIHR MOP 62834 from the Canadian Institutes of Health Research.

* To whom correspondence should be addressed at the Division of Cardiology, McGill University Health Center/Royal Victoria Hospital, H7-17, 687 Pine Ave. West, Montreal, QC, Canada H3A 1A1. Phone (514) 842-1231, ext 34642; fax (514) 843-2813; e-mail jacques.genest@muhc.mcgill.ca.

‡ Royal Victoria Hospital and McGill University Health Centre.

§ Fukushima Medical University School of Medicine.

|| Institut de recherches cliniques de Montreal.

⊥ Cell Map Laboratory, McGill University.

[1] Abbreviations: ASM, acid sphingomyelinase; EDTA, ethylenediaminetetraacetic acid; ER, endoplasmic reticulum; HA, hemagglutinin; HEPES, *N*-(2-hydroxyethyl)piperazine-*N*′-ethanesulfonic acid; IBMX, isobutyl methylxanthine; NPD-A/B, Niemann−Pick disease, type A/B; PBS, phosphate-buffered saline; PMA, phorbol myristate acetate; PMSF, phenylmethanesulfonyl fluoride; PVDF, poly(vinylidene difluoride); SDS−PA(G)GE, sodium dodecyl sulfate−polyacrylamide (gradient) gel electrophoresis; SM, sphingomyelin; SMPD-1, sphingomyelin phosphodiesterase 1; YFP, yellow fluorescent protein.

10.1021/bi700817g CCC: $37.00
Published on Web 12/01/2007

increase in cholesterol due to defects in ASM could lead to impairment of many other normal cellular functions. Furthermore, it has been recently shown by Tabas and coworkers (*12*) and by our group (*13*) that ASM is possibly an important key player in plasma lipoprotein metabolism and thus modulates the susceptibility to atherogenesis.

The emerging functions for the biologically active sphingolipids have therefore underscored the importance of a better understanding of the ASM protein. It will help elucidate the mechanism of ASM functions and unveil the complex pathways of sphingolipid metabolism, as well as increase the understanding of the nature of the phenotypic variations in sphingolipid storage disorders or in cancers. Human ASM was first described in the late 1960s (*14*, *15*) and subsequently purified from a variety of sources (*16*, *17*). However, its full-length cDNA and genomic sequences were isolated and characterized only in 1992 by Schuchman et al. (*18*). Although the SMPD-1 gene was cloned, there was very little molecular and structural information of the protein available. ASM is formed by 629 amino acids with a predicted molecular mass of ~70 kDa. On the basis of structure and motif prediction analyses (*19*−*21*), ASM belongs to the metallophosphoesterase family that includes a diverse range of phosphoesterases, including protein phosphoserine phosphatases, nucleotidases, and 2′,3′-cAMP phosphodiesterases. Its predicted catalytic domain spans from amino acid 199 to 461, as illustrated in Figure 1. The ASM protein also contains a signal peptide at the N-terminal region and a saposin B domain (amino acid 87−165), which appears to serve as activator in the lipid degradation (*22*). The peptide sequence is also spanned by six *N*-glycosylation sites, 10 putative phosphorylation sites, and six disulfide bonds (*23*). Site-directed mutagenesis has revealed that five of these sites were used (*24*) and mass spectrometry has confirmed the presence of the disulfide bonding (*25*). A detailed crystal structure of ASM is not yet available, but its prediction has been recently attempted on the basis of its similarity to purple acid phosphatase (1ute) by using comparative modeling (*26*). However, this prediction model shares a sequence identity of only <15% of the template, and the C-terminal region of ASM was excluded.

Analyses of SMPD-1 sequence in families with NPD have led to the identification of over 100 NPD-A (severe phenotype) and NPD-B (milder phenotype) mutations (*27*−*30*). These mutations span all across the protein peptide sequence. Surprisingly, the C-terminal region harbored the second highest number of mutations after the catalytic domain. It also includes ΔR608, which represents one of the most prevalent NPD mutations (*31*). Although this C-terminal region from amino acids 490−620 does not hold a recognizable functional domain or motif, it contains some important posttranslational modification sites (Figure 1). Substitution or deletion of these C-terminal residues might substantially alter the structure as well as affect the catalytic ability or efficiency of SM hydrolysis. Therefore, the C-terminal region of ASM seems to be important despite the lack of any known functions. Nonetheless, full information on the structure and function of ASM is still lacking in the literature. The essential features governing its catalytic activity remain unknown.

Herein, we dissected the structure and functions of the C-terminal region (N490−N629) of ASM and demonstrated

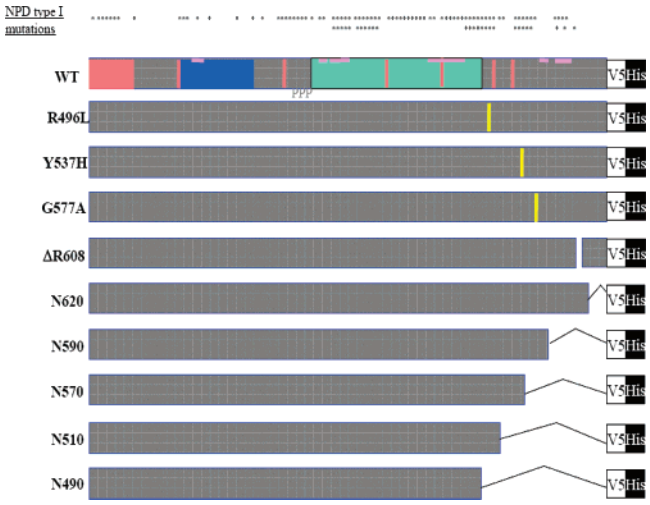

FIGURE 1: ASM sequence and mutagenesis. ASM is a relatively small protein (629 amino acids with a theoretical molecular mass of 70 kDa) consisting of a signal peptide (amino acids 1−46) in the N-terminal region (in red), a small transmembrane domain (amino acids 25−47) (in yellow), a saposin B region (amino acids 87−165) (in blue) that serves as an activator of various lysosomal lipid-degrading enzymes, a proline-rich region (amino acids 179−197) (as black P), followed by the metallophosphoesterase catalytic domain (amino acids 199−461) (in green). In addition, the ASM contains six glycosylation sites [five of which are used according to Ferlinz et al. (*26*)], six disulfide bonds, and multiple highly putative phosphorylation sites. NPD type A or B mutations [summarized by Sikora et al. and Simonaro et al. (*29*, *30*)] were discovered throughout the entire protein. Interestingly, the C-terminal region of the ASM harbors the second highest number of mutations (29 in total), many of which lead to severe enzymatic defects. The ΔR608 within this region is one of the most prevalent NPD mutations (*33*) and is also the mutation that we have discovered in the kindred under our investigation (*34*). Glycosylation sites are indicated as orange vertical lines; disulfide bonds are drawn as pink horizontal lines. Five serial deletion mutants are designed such that the entire C-terminal region (amino acids 462−629) is spanned: N620 has the smallest deletion and retains all posttranslational modification sites in the C-terminus. N590 conserves all posttranslational modification sites except the sixth disulfide bonding sites (C594−C607). N570 lacks both the fifth (C584−C588) and sixth (C594−C607) disulfide bonding sites. N510 excludes the sixth glycosylation site (N520) in addition to the loss of the two disulfide bonds. N490 retains only the 28 amino acids adjacent to the catalytic domains, missing all posttranslational modification sites in the C-terminus. Point mutants (indicated as vertical yellow lines) R496L, Y537H, and G577A are naturally occurring NPD-A mutants that are known to have severely defective enzymatic function. ΔR608 is a naturally occurring NPD-−B mutant.

that this region, narrowed down to the minimal 30 amino acids (N590−N620) containing the sixth disulfide bond, significantly contributed to the overall conformational integrity dictating its enzymatic functions and secretion. The information in this report should prove useful for future studies that explore the enzymology, regulation, and functions of ASM as well as the pathophysiology related to different SMPD-1 gene defects.

MATERIALS AND METHODS

Materials. All tissue culture media and transfection reagents were from Invitrogen (Carlsbad, CA). Chinese hamster ovarian (CHO) cells and *Spodoptera frugiperda sf*9 cells as well as their culture medium and transfection reagents were from Invitrogen (Carlsbad, CA); *Cercopithecus aethiops*

(COS-7) cells were from the American Type Culture Collection (Manassas, VA). Primary skin fibroblasts were prepared from a compound heterozygous Niemann−Pick disease type B (NPD-B) patient (ΔR608 and R441X) as we have previously described (*32*). Precast 10% Tris−glycine gels were from Mirador DNA Design (Montreal, QC). β-Galactosidase assay kits were from Promega (Madison, WI). Quikchange II site-directed mutagenesis kits and cloning reagents were from Stratagene (La Jolla, CA). Mouse anti-V5 antibodies were from Invitrogen (Carlsbad, CA), rat anti-HA monoclonal antibodies were from Roche Applied Sciences (Indianapolis, IN), and rabbit anti-YFP polyclonal and mouse anti-KDEL monoclonal antibodies were a generous gift from Dr. Wada, Fukushima Medical University, Japan. Horseradish peroxidase-conjugated rabbit anti-mouse antibodies and PVDF were from GE Healthcare Bio-Sciences (Piscataway, NJ). Mouse anti-mono/polyubiquitinated proteins (clone FK2), S5a agarose, and ubiquitin aldehyde were from Biomol International (Plymouth Meeting, PA). Magnetic beads for small-scale His-tagged protein purification by immobilized metal affinity chromatography were from Dynal Biotech (Brown Deer, WI). Protein A beads for immunoprecipitation were from either Miltenyi Biotec (Auburn, CA) or GE Healthcare Bio-Sciences (Piscataway, NJ). β-Endo-*N*-acetyglucosaminidase H (endoH) and peptide-N- glycanase F (PNGase F) were from New England Biolabs (Ipswich, MA). [^{3}H]Sphingomyelinase scintillation proximity assay kits were from GE Healthcare Bio-Sciences (Piscataway, NJ). Sphingomyelin, phosphatidylcholine, and other lipids were from AvantiLipids (Alabaster, AL). All other chemicals were from Sigma (St. Louis, MO).

Construction of Mammalian Expression Plasmids and Cell Culture. Mammalian cell culture was maintained in DMEM containing 5−10% fetal bovine serum, 0.1 mM nonessential amino acids, with or without penicillin/streptomycin. CHO or COS cells were transciently transfected with wild-type or mutant ASM cDNAs with lipofectamine 2000 (Invitrogen, Carlsbad, CA) according to the manufacturer's instructions. In some cases, β-galactosidase cDNA (pCMVβ) was cotransfected to control transfection efficiency. Mutagenesis of the pcDNA3.1/GS wild-type ASM (Invitrogen, Carlsbad, CA) was performed with Quickchange II Mutagenesis kit (Stratagene, La Jolla, CA). The authenticity of all mutants was confirmed by nucleotide sequencing.

Immunoblot, Immunoprecipitation, and Protein Purification. For expression study, cell lysates were harvested 24 h after transfection and prepared with 1% Triton X-100 lysis buffer (150 mM NaCl, 1% Triton X-100, 50 mM Tris-HCl, pH 8.0, with EDTA-free protease inhibitor cocktails, Roche Applied Sciences, Indianapolis, IN). The cellular homogenates were then assayed for β-galactosidase activity for transfection efficiency control. Conditioned medium was collected, spun at 800 g for 15 min to pellet any contaminating cells, and concentrated down to ≤1 mL by use of a Centriprep 30 concentrator (Amicon, Beverly, MA). Cell lysates or concentrated medium were mixed with bromophenol blue-containing loading buffer, boiled, and directly loaded on 10% Tris−glycine SDS−PAGE after normalization with the transfection efficiency. Gels were then electrotransferred to PVDF for immunoblotting. Blots were incubated with 5% dry milk and various primary and horseradish peroxidase-conjugated secondary antibodies. Finally, the blots were soaked in chemiluminescence reagent (Pierce, Rockford, IL) and exposed to Omat-Blue X-ray films.

For other experiments, the His/V5-tagged ASM was first purified by metal affinity chromatography or, alternatively, immunoprecipited with protein A−Sepharose and different antibodies. In ubiquitination studies, lysis buffer containing *N*-ethylmaleimide (NEM) and ubiquitin aldehyde (50 mM HEPES, pH 7.5, 5 mM EDTA, 150 mM NaCl, 1% Triton X-100, EDTA-free protease inhibitors cocktail, 10 mM NEM, and 100 nM ubiquitin aldehyde) was used to lyse the cells treated with epoxomicin (25 mM, Calbiochem, San Diego, CA). Polyubiquitinated proteins were purified by S5a-affinity chromatography as previously described (Biomol International, Plymouth Meeting, PA) (*33*). After electrophoresis and transfer, membranes were preincubated in denaturing buffer (6 M guanidine hydrochloride, 20 mM Tris-HCl, pH 7.5, 5 mM β-mercaptoethanol, and 1 mM PMSF) for 1 h at 4 °C followed by extensive PBS washing before anti-FK2 antibody incubation. Immunoblots were performed as described above.

Cell Surface Biotinylation. Surface proteins were biotinylated with 500 μg/mL sulfosuccinimido 2-(biotinamido)-ethyl-1,3-dithiopropionate (Pierce) for 30 min at 4 °C. The biotinylation reaction was quenched for 10 min at 4 °C by addition of 1 M Tris-HCl (pH 7.5) to the reaction mixture to a final concentration of 20 mM. Cells were washed twice with ice-cold PBS, lysed, and homogenized. Protein (200 μg) was added to 30 μL of streptavidin−Sepharose beads, and the mixture was incubated overnight on a platform mixer at 4 °C. The pellet (plasma membrane; PM) was separated on SDS−PAGGE (4−22.5%) and ASM associated with the PM was detected with the appropriate antibody.

Sphingomyelinase Assay. ASM activity was assessed by the scintillation proximity assay. The standard 100 μL assay mixture consisted of up to 40 μL of sample (cell lysates, conditioned medium, or immunoprecipitates) and 0.1 M sodium acetate assay buffer, pH 5.0, with or without 0.1 M Zn^{2+}, and 0.625 pmol of [^{3}H]biotinylated SM substrate. The assay mixtures were incubated at 37 °C for 1 h and the reactions were stopped by the addition of streptavidin−scintillation beads. Only nonhydrolyzed [^{3}H]SM could be precipitated by the beads and detected by β-counter, thus the radioactivity was inversely related to the amount of SM hydrolyzed.

Immunofluoresence Localization Study. The sorting fate of the wild-type and mutant ASM was monitored by confocal microscopy. After 16-h transient transfection in the absence or presence of anti-protease inhibitors (leupeptin and pepstatin) or cyclohexamide, cells were washed, fixed, and permeabilized with methanol. They were then immunostained with mouse anti-V5 primary antibodies (Invitrogen, Carlsbad, CA) and Alexa Fluor 546 rabbit anti-mouse secondary antibody (absorbance 556 nm, emission 573 nm; Invitrogen, Carlsbad, CA). In colocalization studies, cells were treated with Lysotracker for 30 min before cell harvest (Molecular Probes, Eugene, OR) or co-immunostained with various organelle markers labeled with Oregon Green 488 goat anti-rabbit secondary antibody (absorbance 496 nm, emission 524 nm; Invitrogen, Carlsbad, CA). In all experimental conditions, cells on each coverslip were photographed in multiple fields and appropriate negative controls were used. In separate experiments, wild-type ASM as well as ΔR608 and

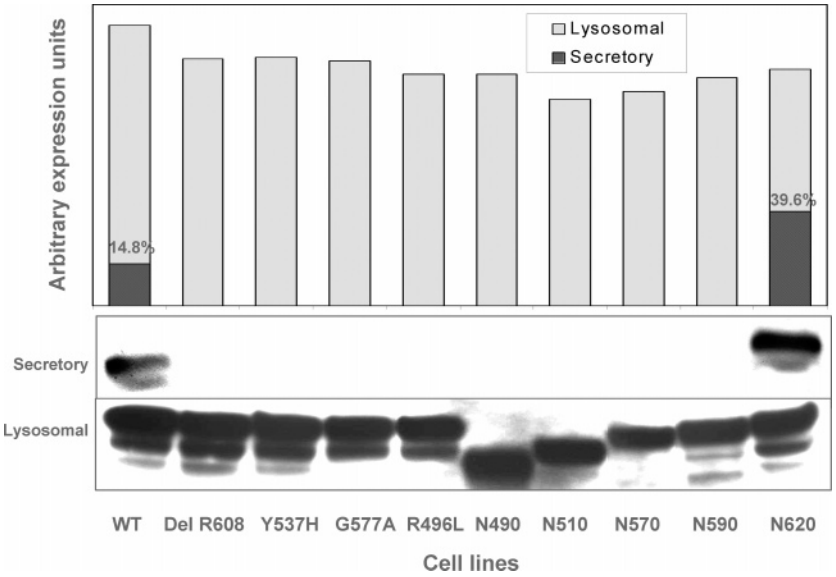

FIGURE 2: Protein expression of wild-type and mutant ASM in cell and in medium. After 24 h, cotransfection of pcDNA3.0/GS-SMPD-1 and pCMVb β-gal in subconfluent CHO cells grown in 10-cm dishes, 1 mL of total cell lysates was harvested and 20 μL of this latter was used in the immunoblot analyses to study the expression of wild-type and mutant lysosomal ASM. The total medium (15 mL) was also harvested and concentrated with Amicon Ultra 15 (MW cutoff 30 000) down to 1 mL in volume. An aliquot (20 μL) of this latter was used in the immunoblot analyses to study the expression of wild-type and mutant secretory ASM. The immunoblots for both lysosomal and secretory expression were handled in parallel with identical experimental conditions as following: anti-V5 primary antibodies were used against the recombinant ASM, while streptavidin-conjugated monoclonal rabbit anti-mouse secondary antibodies were used for subsequent detection. The bands in the blots exposed for 1 min were quantified by use of AlphaImager, normalized by the transfection efficiency assessed by β-galactosidase assay, and plotted for the calculation of the ratio between secretory (upper lane) and lysosomal (lower lane) expression levels.

N590 mutants were subcloned into N-terminally YFP- or HA-tagged vectors, and their localization was examined by use of polyclonal anti-YFP and monoclonal anti-HA antibodies, respectively (*34*).

Statistics. All experiments were independently repeated 3−5 times. When applicable, results were given as means ± SD ($n = 3$).

RESULTS

Normal Expression yet Defective Secretion in ASM Mutants. In order to study the role of the C-terminal region of ASM protein, four naturally occurring mutations and five serial deletions were created as illustrated in Figure 1. The protein expression of all nine mutants was assessed. We found that all of them, including N490 with a deletion of 139 amino acids, were properly expressed in the cells (Figure 2). The SDS−PAGE analysis revealed that the His/V5-tagged wild-type ASM migrated as a single band with an apparent molecular mass of ~72 kDa, similar to the previously reported FLAG-ASM (*35*). Occasionally, a minor faster-migrating band appeared, representing the protease-induced degradation products (*36*). Like many lysosomal proteins, the same SMPD-1 gene gives rise to both lysosomal and secretory ASM (*37*). The secreted wild-type ASM characterized in this paper had a molecular mass of ~75 kDa (Figure 2) and represent less than 15% of total cell ASM, consistent with a previous study (*4*). The more rapid migration of the lysosomal ASM on SDS−PAGE compared to the secretory ASM was due both to proteolytic processing and to differences in oligosaccharide structure (Supporting Information). Surprisingly, while the cellular expression of the mutants was comparable to that of the wild-type ASM, we observed a quasi-absence of mutant ASM in medium, except for N620, the mutant that has the smallest deletion and that preserves all post-translational modification sites. The secretion defects in mutant ASM were also confirmed in *Sf*21 insect models (Supporting Information), for which we have generated wild-type and mutant ASM baculovirus transfer vectors using the Gateway BaculoDirect baculovirus expression system (Invitrogen, Carlsbad, CA) as detailed in Rabah et al. (*38*) and Bartelsen et al. (*39*). Since the protein expression was normal, the lack of secreted mutant ASM appeared to be caused by hindrance either in the transit through the ER after the protein synthesis or during the trafficking through the Golgi secretory pathway.

Enzymatic Activity of Mutant ASM Was Severely Abolished. Although all ASM mutants have normal cellular expression, we speculated that their enzymatic function may not be preserved, at least for the largest deletion mutants and the four naturally occurring mutants known to be inactive in patients with Niemann−Pick disease types A and B. As expected, the truncations in the four deletion mutants and the mutations in the four naturally occurring mutants led to total inactivation of ASM (Figure 3). Importantly, instead of observing a gradual decrease in activity as increasing numbers of residues were deleted from the C-terminus, we revealed that the only mutant that conserves intact ASM activity was N620, the smallest deletion mutant that has only 9 amino acids deleted from its C-terminal end (Figure 1). Interestingly, this pattern of loss of function in the lysosomal mutant ASM is closely related to impaired secretion (Figure 2). Thus, it is clear that the C-terminus of ASM plays an important role in structure−function yet to be characterized. In effect, we could narrow down to the minimal region from amino acids 590 to 620 that appear to be essential to safeguard the enzymatic function and protein secretion.

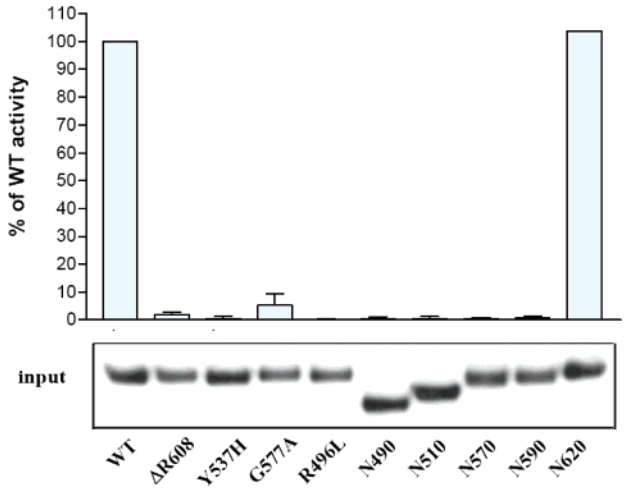

FIGURE 3: ASM mutant enzymatic activity. Recombinant ASM proteins were pulled down by magnetic immobilized metal affinity chromatography. The purified enzymes were incubated with [^{3}H] biotinylated SM for 1 h at 37 °C. The enzymatic reaction was stopped with streptavidin-coated yttrium silicate beads and counted. The enzymatic activity was imversely proportional to the counted cpm. The uniformity of the input in the enzymatic activity assay was assessed by monoclonal anti-V5 primary antibodies and monoclonal rabbit anti-mouse secondary antibodies.

Accordingly, only the ΔR608 and N590 mutants were used for all subsequent experiments.

The ASM activity was also examined in conditioned medium, and an identical abolished activity pattern was found in the same mutants (data not shown). Although their functional inactivation was highly plausible, this lack of SM hydrolysis by the secreted mutant ASM was likely to be caused by their barely detectable levels in the medium (Figure 2). In order to exclude the possibility of an "enzyme secretion−recapture" mechanism that some believed to play a role in enzyme processing and activation (*40*), excess receptor-specific ligands mannose 6-phosphate (10 mM) (*41*) were loaded onto CHO cells transfected with wild-type ASM cDNA in order to compete for the receptor binding and to inhibit protein reuptake. Our data indicated that the blockade of the cell-surface mannose phosphate receptors by free mannose inhibiting the reinternalization of the secreted ASM did not affect the cellular wild-type ASM function (data not shown). Therefore, this mechanism could not be a plausible explanation for the functional inactivation in ASM mutants. This result was consistent with the finding in the report by von Figura and Weber (*42*), who provided evidence that secretion−recapture plays a minor role in the targeting and maturation of newly synthesized lysosomal enzymes. Furthermore, recent studies confirmed that ASM, like many other lysosomal proteins, also uses mannose 6-phosphate-independent targeting system to reach the lysosomal compartments (*43*).

ER Entrapment of Mutant ASM. Defects in secretion and functions indicated that the ASM mutants were most likely trapped in the ER quality control machinery. We examined by confocal microscopy the intracellular localization of the C-terminally V5-tagged wild-type and mutant recombinant ASM subsequent to a 16-h transient transfection in COS cells. While we found that ΔR608 and N590 were trapped in the ER as predicted, we also observed ER-localized fluorescence for the wild-type ASM (data not shown). ASM is known to be located in the lysosomal compartments, and this observation could be explained by two possibilities: (1) The C-terminus of the ASM may be cleaved after reaching the lysosomal compartment, as seen with other lysosomal proteins. Thus, the V5 tag may be cleaved in mature ASM such that the anti-V5 antibodies could only detect the unprocessed wild-type ASM that remains in the ER compartments. (2) Alternatively, the overexpression system overloaded the protein biosynthesis machinery such that many of the overexpressed ASM proteins remained unprocessed and entrapped in the ER after protein translation.

To validate our aforementioned observations and premises, we have separately subcloned the wild-type and mutant ASM into N-terminally YFP- and HA-tagged vectors. We also suppressed protein overproduction by treating the cells with cyclohexamide. As shown in Figure 4, we consistently found that the ΔR608 and N590 mutants were localized in the ER; the presence or absence of protease inhibitors did not alter this distribution (*44*). The strong fluorescence signals also supported an expression (Figure 2) and half-life (Supporting Information) comparable to that of wild type. In contrast, under these new experimental conditions, we could clearly observe the lysosomal fluorescence in wild-type ASM-transfected cells that were colocalized with lysosomal but not ER markers (Figure 4). This is consistent with our finding that mutant ΔR608-transfected CHO cells and fibroblasts from a compound heterozygous Niemann−Pick disease type B (NPD-B) patient (ΔR608 and R441X) (*32*) have defective translocation of the enzyme to the plasma membrane (PM) (Figure 5). Our confocal and cell surface biotinylation data, together with the results from the secretion and enzymatic assays, strongly suggested that the C-terminal mutations led to aberrant structural folding and important functional defects that prevent the mutant proteins from trafficking through the ER quality control checkpoint and their translocation to the PM.

Ubiquitinated Mutant ASM Was Found in the Cells. Proteins that fail to pass the ER are eventually eliminated by ubiquitination and proteosomal degradation. In order to further examine the impact of mutations in the ASM C-terminus, we studied the ubiquitination of the N590 and ΔR608 mutants by pull-down with S5a-agarose from total cell lysates prepared with epocimycin and ubiquitin aldehyde. S5a is a subunit of the 19S regulator of the 26S proteosome that has been shown to bind multiubiquitinylated proteins containing chains of at least four ubiquitin moieties (*45*). As predicted from their ER localization, we revealed that while there was little steady-state ubiquitinated wild-type ASM in the cells, there was a substantial amount of high-molecular weight polyubiquitinated mutant ASM (Figure 6). The ubiquitination of the mutants was concomitantly confirmed by immunoprecipitation with anti-V5 followed by immunoblotting with anti-mono/polyubiquitinated protein antibodies. Interestingly, we also observed an ubiquitinated form of ASM with an apparent molecular mass of ∼50 kDa. This band has previously been characterized in the initial molecular cloning and characterization of ASM (*24*), even though its role and functionality remained elusive. Our observation that this molecular form was highly ubiquitinated and was barely detectable indicated that it was likely an alternately processed isoform (reported to constitute ≤10%

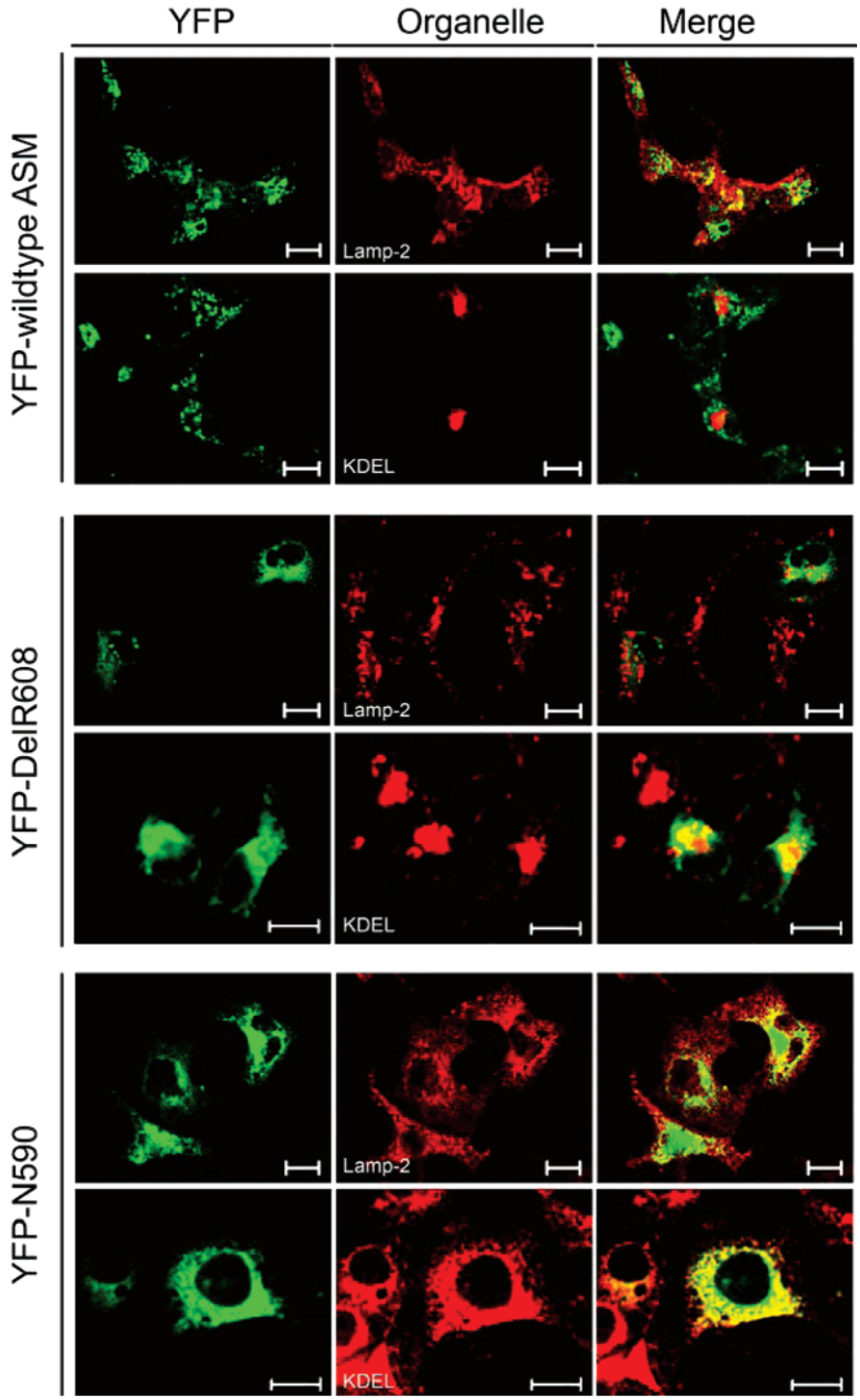

FIGURE 4: ASM mutant entrapment in the ER. COS cells grown on coverslips were transciently transfected with N-terminally YFP-tagged wild type and ΔR608 and N590 mutant ASM for 10 h in the presence of leupeptin (10 μg/mL) and pepstatin (10 μg/mL), followed by an incubation with cyclohexamide for an additional 6 h. Cells were fixed with methanol for 10 min at −20 °C and washed with immunostaining blocking buffer for 20 min. After being labeled with rabbit anti-YFP polyclonal antibodies (1:400) and mouse anti-lamp2 (lysosomal markers, 1:100) or anti-KDEL (ER markers, 1:100) monoclonal antibodies for 20 min, the cells were washed and further labeled with Oregon Green 488 goat anti-rabbit and Alexa Fluor 546 anti-mouse secondary antibodies. Scale bar = 20 μm.

of ASM product) (*46*) that was catalytically inactive and was usually degraded rapidly.

DISCUSSION

The role of the C-terminus in the secretion has been described in other lysosomal proteins. For example, Chauhan et al. (*47*) and Claveau et al. (*48*) have independently demonstrated the involvement of the C-terminal amino acids in the secretion of human lysosomal protease cathepsin L. Our data are consistent with the concept that the functional integrity of a protein is governed by its tertiary and quaternary structures and not solely by an intact catalytic domain. In ASM, the predicted catalytic site lies in the amino acids 199−461. The activity of all truncation mutants illustrated that the removal of a 30-minimal amino acid region in the C-terminus (amino acids 590−620) was

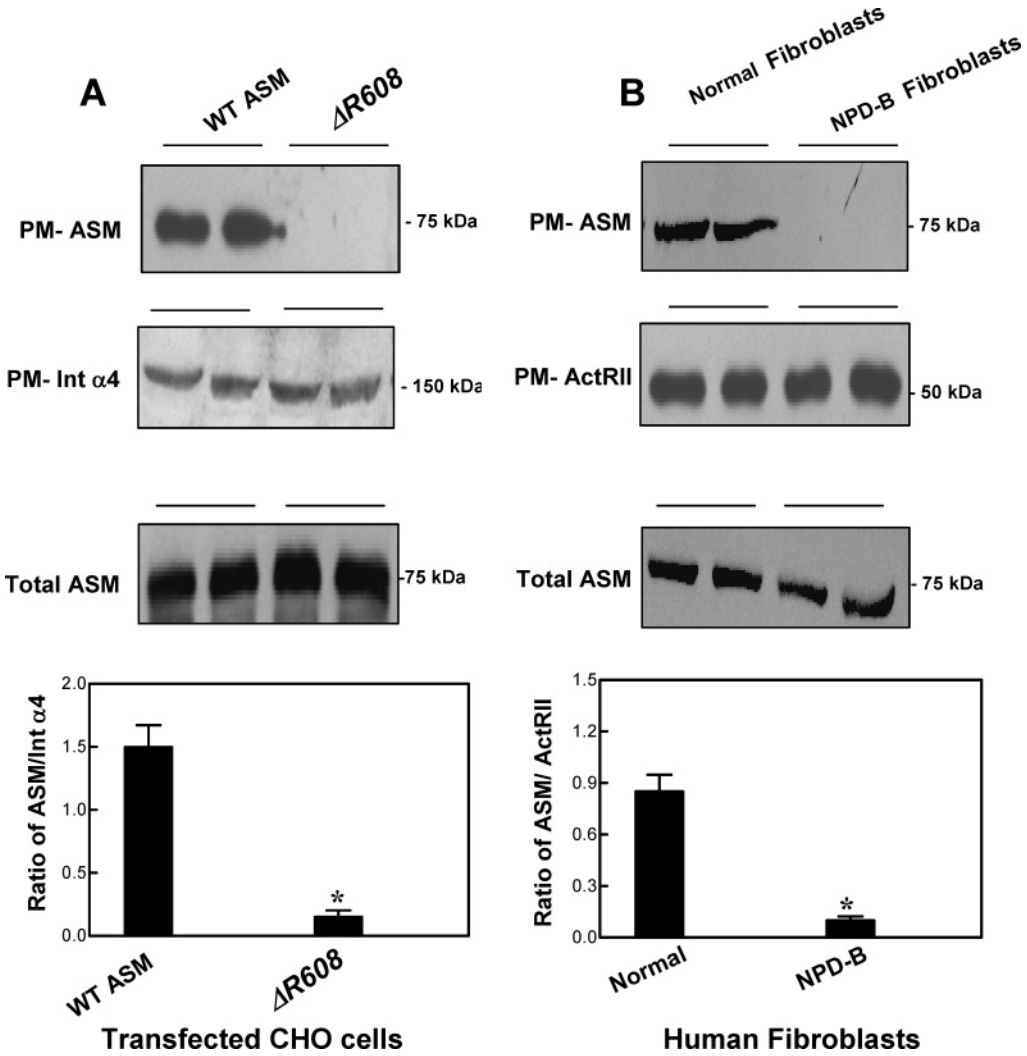

FIGURE 5: ASM mutation ΔR608 impairs the translocation of the enzyme to the plasma membrane in transfected CHO cells and NPD-B fibroblasts. Transfected CHO cells (A) and fibroblasts from NPD-B subjects (B) were subjected to cell surface biotinylation as described under Materials and Methods. Cells were washed twice with ice-cold PBS, lysed, and homogenized, and 200 μg of protein was added to 45 μL of streptavidin−Sepharose beads and incubated overnight on a platform mixer at 4 °C. The PM samples or total cell lysates were separated by SDS−PAGGE. Transfected ASM in CHO cells was revealed by anti-V5 primary antibodies as described above. ASM associated with the PM or total cell ASM in NBD-B fibroblasts was detected by polyclonal human anti-ASM antibody (Santa Cruz). Integrin α4 (Int α4) and activin recptor type (ActRII) associated with the PM samples were detected with appropriate antibodies and were used as controls for protein loading. The ratios of PM-ASM to Int α4 and of PM-ASM to ActRII were quantitated by densitometric scanning. Results shown are representative of two independent experiments. *$p < 0.001$ by Student's t test.

sufficient to inactivate the enzyme, implying the crucial role of this C-terminal region even though it apparently does not harbor recognizable domains or motifs.

The misfolding of ΔR608 and N590 C-terminal ASM mutants was not unpredictable on the basis of the location of their deletion/truncation (Figure 7): the former has one arginine deletion at position amino acid 608, immediately adjacent to the cysteine residue at position 607 that has been shown to form one of the six disulfide bonds in ASM (*25*). Similarly, the only difference between the inactive N590 mutant and active N620 mutant (which conserves 100% of the ASM activity) was the deletion of this same disulfide bond. Disulfide bonds play crucial roles in the tertiary conformation of a protein (*49*). The peculiarity of the cysteine residues in the ASM C-terminus was once reported by Qiu et al. (*50*), who activated the ASM by deleting the terminal free thiol (cysteine^{629}). They explained the observation by a "cysteine switch mechanism", which is coordinated by the free cysteine along with other cysteine residues structurally paired in disulfide bonds. The precise coordination and association of both free and bonded cysteines, especially when they are in close proximity, appear critical, as any disarrangement could lead not only to activation but also to inactivation (as shown in Figure 3), as well as disulfide shuffling causing intermolecular cross-links and ER retention (*51*). Although the precise mechanism by which the C-terminal mutations impact the function and structure of ASM has not been defined in this paper, we believe that this was a consequence of a significant alteration in the tertiary conformation brought about by the absence of an important disulfide bond. Importantly, our finding that C-terminal mutations impaired the trafficking of mutant enzymes as described in the present heterologous overexpression system was strongly supported by our observation that a naturally occurring mutation (ΔR608) associated with NPD-B (Figure 5) had defective translocation to the plasma membrane.

Posttranslational modifications such as glycosylation and phosphorylation are commonly affected when a protein is

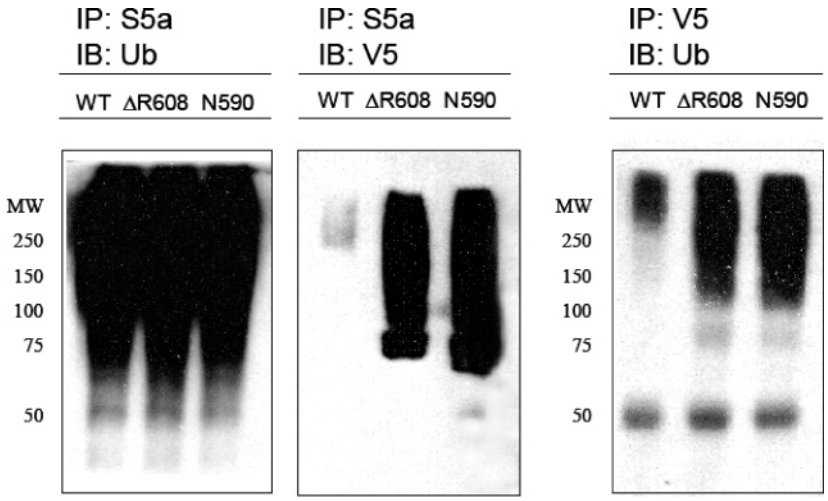

FIGURE 6: ASM mutant ubiquitination. Wild-type and mutant ASM proteins were pulled down by either S5a-agarose (left panels) or by anti-V5 antibodies (right panels). The precipitated samples were then revealed by anti-ubiquitin or anti-V5 antibodies. The blot on the left (IP: S5a/ IB: Ub) was a control for the pull down of ubiquitinated proteins by S5a-agarose. The blots in the middle (IP: S5a/ IB: V5) and on the right (IP: V5/ IB: Ub) concomitantly demonstrated the presence of increased levels of mutant ASM in ubiquinated forms.

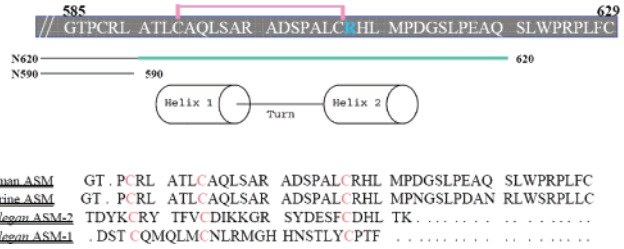

FIGURE 7: Amino acid sequence alignment of human ASM C-terminus with ASM homologues from different species. Within the C-terminal 30-amino acid region of ASM (amino acids 590−620), there is a disulfide bond involving a cysteine residue at position 607and a 20-amino acid long helix−loop−helix pattern that contains 12 nonpolar and four charged residues. The human ASM shared 81% homology with the murine counterpart. Although it is only 30% homologous to the *Caenorhabditis elegans* ASM-1 and ASM-2, its cysteine residues within this region are well conserved, hinting the importance of the disulfide bond for the structural conformation.

misfolded. The wild-type ASM has 10 putative phosphorylation sites in the C-terminal region, but its phosphorylation status has never been demonstrated. Our preliminary data showed that the wild-type ASM was not phosphorylated even when stimulated with PMA (*52*), forskolin (*53*), or IBMX (*54*) and that its phosphorylation was solely derived from its mannose 6-phosphate moieties (Supporting Information). Surprisingly, we found that the ΔR608 and N590 mutant ASM were phosphorylated even under basal conditions (Supporting Information). We speculate that the structural alterations made those phosphorylation sites in mutants ASM accessible for kinases. In addition, we have found a significant amount of mutant aggregates revealed under nonreducing conditions (Supporting Information). It is commonly believed that aggregates were caused by aberrant interchain disulfide bonds and that they are often abnormally phosphorylated (*55*). Intriguingly, Zeidan and Hannun (*56*) have recently published their findings on ASM phosphorylation. While different experimental systems and conditions could explain the discrepancies, more in-depth investigation as well as characterization by methods such as circular dichroism and X-ray crystallography will be necessary in the future to better elucidate the ASM structure.

Our structure−function study in ASM significantly contributed to the mechanistic elucidation of how specific mutations could affect its biological function, whether it involves the catalytic ability, affinity to cofactor, secretion, or substrate binding. We have demonstrated here that the C-terminus of ASM contains a 30-amino acid sequence essential for at least one of these functions. Current research has shown that defects in ASM could lead to Niemann−Pick diseases and disturbance in lipid/lipoprotein metabolism as well as deregulation in many signaling cascades regulating apoptosis (*57*, *58*). Therefore, a better understanding of its structure will enable us to more efficiently and accurately predict the severity of a SMPD-1 mutation under these pathophysiological conditions and to find potential therapeutic strategies.

SUPPORTING INFORMATION AVAILABLE

ASM wild-type and mutant glycosylation (Figure 1S), ASM mutant secretory defects in Sf21 insect models (Figure 2S), ASM wild-type and mutant half-life (Figure 3S), and ASM mutant aberrant phosphorylation and aggregation (Figure 4S). This material is available free of charge via the Internet at http://pubs.acs.org.

REFERENCES

1. Merrill, A. H., Jr., and Jones, D. D. (1990) An update of the enzymology and regulation of sphingomyelin metabolism, *Biochim. Biophys. Acta 1044*, 1−12.
2. Scriver, C. R., Beaudet, A. L., Sly, W. S., Valle, D., Childs, B., Kinzler, K. W., and Vogelstein, B., Eds. (2001) *The Metabolic & Molecular Bases of Inherited Disease*, Vol. III, 8th ed., pp 3371−3894, McGraw-Hill, New York.
3. Schuchman, E. H., Levran, O., Pereira, L. V., and Desnick, R. J. (1992) Structural organization and complete nucleotide sequence of the gene encoding human acid sphingomyelinase (SMPD1), *Genomics 12*, 197−205.
4. Schissel, S. L., Schuchman, E. H., Williams, K. J., and Tabas, I. (1996) Zn2+-stimulated sphingomyelinase is secreted by many cell types and is a product of the acid sphingomyelinase gene, *J. Biol. Chem. 271*, 18431−18436.
5. Brady, R. O., Kanfer, J. N., Mock, M. B., and Fredrickson, D. S. (1966). The metabolism of sphingomyelin. II. Evidence of an enzymatic deficiency in Niemann-Pick disease, *Proc. Natl. Acad. Sci. U.S.A. 55*, 366−369.

6. Ion, G., Fajka-Boja, R., Kovacs, F., Szebeni, G., Gombos, I., Czibula, A., Matko, J., and Monostori, E. (2006). Acid sphingomyelinase mediated release of ceramide is essential to trigger the mitochondrial pathway of apoptosis by galectin-1, *Cell. Signalling 18*, 1887−1896.
7. Kolesnick, R., and Fuks, Z. (2003) Radiation and ceramide-induced apoptosis, *Oncogene 22*, 5897−5906.
8. Pozo, D., Vales-Gomez, M., Mavaddat, N., Williamson, S. C., Chisholm, S. E., and Reyburn, H. (2006) CD161 (human NKR-P1A) signaling in NK cells involves the activation of acid sphingomyelinase, *J. Immunol. 176*, 2397−2406.
9. Wong, M. L., Xie, B., Beatini, N., Phu, P., Marathe, S., Johns, A., Gold, P. W., Hirsch, E., Williams, K. J., Licinio, J., and Tabas, I. (2002) Acute systemic inflammation up-regulates secretory sphingomyelinase in vivo: a possible link between inflammatory cytokines and atherogenesis, *Proc. Natl. Acad. Sci. U.S.A. 97*, 8681−8686.
10. Leventhal, A. R., Chen, W., Tall, A. R., and Tabas, I. (2001) Acid sphingomyelinase-deficient macrophages have defective cholesterol trafficking and efflux, *J. Biol. Chem. 276*, 44976−44983.
11. Ridgway, N. D., Byers, D. M., Cook, H. W., and Storey, M. K. (1999) Integration of phospholipid and sterol metabolism in mammalian cells, *Prog. Lipid Res. 38*, 337−360.
12. Marathe, S., Kuriakose, G., Williams, K. J., and Tabas, I. (1999) Sphingomyelinase, an enzyme implicated in atherogenesis, is present in atherosclerotic lesions and binds to specific components of the subendothelial extracellular matrix, *Arterioscler. Thromb. Vasc. Biol. 19*, 2648−2658.
13. Lee, C. Y., Lesimple, A., Denis, M., Vincent, J., Larsen, A., Mamer, O., Krimbou, L., Genest, J., and Marcil, M. (2006) Increased sphingomyelin content impairs HDL biogenesis and maturation in human Niemann-Pick disease type B, *J. Lipid Res. 47*, 622−632.
14. Schneider, P. B., and Kennedy, E. P. (1967) Sphingomyelinase in normal human spleens and in spleens from subjects with Niemann-Pick disease, *J. Lipid Res. 8*, 202−209.
15. Kanfer, J. N., Young, O. M., Shapiro, D., and Brady, R. O. (1966) The metabolism of sphingomyelin. I. Purification and properties of a sphingomyelin-cleaving enzyme from rat liver tissue, *J. Biol. Chem. 241*, 1081−1084.
16. Quintern, L. E., Weitz, G., Nehrkorn, H., Tager, J. M., Schram, A. W., and Sandhoff, K. (1987) Acid sphingomyelinase from human urine: purification and characterization, *Biochim. Biophys. Acta 922*, 323−336.
17. Lansmann, S., Ferlinz, K., Hurwitz, R., Bartelsen, O., Glombitza, G., and Sandhoff, K. (1996) Purification of acid sphingomyelinase from human placenta: characterization and N-terminal sequence, *FEBS Lett. 399*, 227−231.
18. Schuchman, E. H., Suchi, M., Takahashi, T., Sandhoff, K., and Desnick, R. J. (1991) Human acid sphingomyelinase. Isolation, nucleotide sequence and expression of the full-length and alternatively spliced cDNAs, *J. Biol. Chem. 266*, 8531−8539.
19. Gattiker, A., Gasteiger, E., and Bairoch, A. (2002) ScanProsite: a reference implementation of a PROSITE scanning tool, *Appl. Bioinf. 1*, 107−108.
20. Bateman, A., Coin, L., Durbin, R., Finn, R. D., Hollich, V., Griffiths-Jones, S., Khanna, A., Marshall, M., Moxon, S., Sonnhammer, E. L. L., Studholme, D. J., Yeats, C., and Eddy, S. R. (2004) The Pfam Protein Families Database, *Nucleic Acids Res. Database 32*, 138−141.
21. Gorodkin, J., Heyer, L. J., and Stormo, G. D. (1997) Finding the most significant common sequences and structure motifs in a set of RNA sequences, *Nucleic Acids Res. 25*, 3724−3732.
22. Kolzer, M., Ferlinz, K., Bartelsen, O., Hoops, S. L., Lang, F., and Sandhoff, K. (2004) Functional characterization of the postulated intramolecular sphingolipid activator protein domain of human acid sphingomyelinase, *Biol. Chem. 385*, 1193−1195.
23. CBS Prediction Servers: http://www.cbs.dtu.dk/services/.
24. Ferlinz, K., Hurwitz, R., Moczall, H., Lansmann, S., Schuchman, E. H., and Sandhoff, K. (1997) Functional characterization of the N-glycosylation sites of human acid sphingomyelinase by site-directed mutagenesis, *Eur. J. Biochem. 243*, 511−517.
25. Lansmann, S., Schuette, C. G., Bartelsen, O., Hoernschemeyer, J., Linke, T., Weisgerber, J., and Sandhoff, K. (2003) Human acid sphingomyelinase, *Eur. J. Biochem. 270*, 1076−1088.
26. Seto, M., Whitlow, M., McCarrick, M. A., Srinivasan, S., Zhu, Y., Pagila, R., Mintzer, R., Light, D., Johns, A., and Meurer-Ogden, J. A. (2004) A model of the acid sphingomyelinase phosphoesterase domain based on its remote structural homolog purple acid phosphatase, *Protein Sci. 13*, 3172−3186.
27. Sikora, J., Pavlu-Pereira, H., Elleder, M., Roelofs, H., and Wevers, R. A. (2003) Seven novel acid sphingomyelinase gene mutations in Niemann-Pick type A and B patients, *Ann. Hum. Genet. 67*, 63−70.
28. Simonaro, C. M., Desnick, R. J., McGovern, M. M., Wasserstein, M. P., and Schuchman, E. H. (2002) The demographics and distribution of type B Niemann-Pick disease: novel mutations lead to new genotype/phenotype correlations, *Am. J. Hum. Genet. 71*, 1413−1419.
29. Wasserstein, M. P., Desnick, R. J., Schuchman, E. H., Hossain, S., Wallenstein, S., Lamm, C., and McGovern, M. M. (2004) The natural history of type B Niemann-Pick disease: results from a 10-year longitudinal study, *Pediatrics 114*, 672−677.
30. Dardis, A., Zampieri, S., Filocamo, M., Burlina, A., Bembi, B., and Pittis, M. G. (2005) Functional in vitro characterization of 14 SMPD1 mutations identified in Italian patients affected by Niemann Pick Type B disease, *Hum. Mutat. 26*, 164.
31. Vanier, M. T., Ferlinz, K., Rousson, R., Duthel, S., Louisot, P., Sandhoff, K., and Suzuki, K. (1993) Deletion of arginine (608) in acid sphingomyelinase is the prevalent mutation among Niemann-Pick disease type B patients from northern Africa, *Hum. Genet. 92*, 325−330.
32. Lee, C. Y., Krimbou, L., Vincent, J., Bernard, C., Larramee, P., Genest, J., Jr., and Marcil, M. (2003) Compound heterozygosity at the sphingomyelin phosphodiesterase-1 (SMPD1) gene is associated with low HDL cholesterol, *Hum. Genet. 112*, 552−562.
33. Walters, K. J., Kleijnen, M. F., Goh, A. M., Wagner, G., and Howley, P. M. (2002) Structural studies of the interaction between ubiquitin family proteins and proteasome subunit S5a, *Biochemistry 41*, 1767−1777.
34. Kamada, A., Nagaya, H., Tamura, T., Kinjo, M., Jin, H. Y., Yamashita, T., Jimbow, K., Kanoh, H., and Wada, I. (2004) Regulation of immature protein dynamics in the endoplasmic reticulum, *J. Biol. Chem. 279*, 21533−21542.
35. He, X., Miranda, S. R., Xiong, X., Dagan, A., Gatt, S., and Schuchman, E. H. (1999) Characterization of human acid sphingomyelinase purified from the media of overexpressing Chinese hamster ovary cells, *Biochim. Biophys. Acta 1432*, 251−264.
36. Ferlinz, K., Hurwitz, R., Vielhaber, G., Suzuki, K., and Sandhoff, K. (1994) Occurrence of two molecular forms of human acid sphingomyelinase, *Biochem. J. 301*, 855−862.
37. Schissel, S. L., Keesler, G. A., Schuchman, E. H., Williams, K. J., and Tabas, I. (1998) The cellular trafficking and zinc dependence of secretory and lysosomal sphingomyelinase, two products of the acid sphingomyelinase gene, *J. Biol. Chem. 273*, 18250−18259.
38. Rabah, N., Gauthier, D. J., Gauthier, D., and Lazure, C. (2004) Improved PC1/3 production through recombinant expression in insect cells and larvae, *Protein Expression Purif. 37*, 377−384.
39. Bartelsen, O., Lansmann, S., Nettersheim, M., Lemm, T., Ferlinz, K., and Sandhoff, K. (1998) Expression of recombinant human acid sphingomyelinase in insect Sf21 cells: purification, processing and enzymatic characterization, *J. Biotechnol. 63*, 29−40.
40. Hickman, S., and Neufeld, E. F. (1972) A hypothesis for I-cell disease: defective hydrolases that do not enter lysosomes, *Biochem. Biophys. Res. Commun. 49*, 992−999.
41. Faust, P. L., Wall, D. A., Perara, E., Lingappa, V. R., and Kornfeld, S. (1987) Expression of human cathepsin D in *Xenopus* oocytes: phosphorylation and intracellular targeting, *J. Cell Biol. 105*, 1937−1945.
42. von Figura, K., and Weber, E. (1978) An alternative hypothesis of cellular transport of lysosomal enzymes in fibroblasts. Effect of inhibitors of lysosomal enzyme endocytosis on intra- and extracellular lysosomal enzyme activities, *Biochem. J. 176*, 943−950.
43. Ni, X., and Morales, C. R. (2006) The lysosomal trafficking of acid sphingomyelinase is mediated by sortilin and mannose 6-phosphate receptor, *Traffic. 7*, 889−902.
44. Montenez, J. P., Delaisse, J. M., Tulkens, P. M., and Kishore, B. K. (1994) Increased activities of cathepsin B and other lysosomal hydrolases in fibroblasts and bone tissue cultured in the presence of cysteine proteinases inhibitors, *Life Sci. 55*, 1199−1208.
45. Layfield, R., Tooth, D., Landon, M., Dawson, S., Mayer, J., and Alban, A. (2001) Purification of poly-ubiquitinated proteins by S5a-affinity chromatography, *Proteomics 1*, 773−777.
46. Quintern, L. E., Schuchman, E. H., Levran, O., Suchi, M., Ferlinz, K., Reinke, H., Sandhoff, K., and Desnick, R. J. (1989) Isolation

of cDNA clones encoding human acid sphingomyelinase: occurrence of alternatively processed transcripts, *EMBO J. 8*, 2469−2473.
47. Chauhan, S. S., Ray, D., Kane, S. E., Willingham, M. C., and Gottesman, M. M. (1998) Involvement of carboxy-terminal amino acids in secretion of human lysosomal protease cathepsin L, *Biochemistry. 37*, 8584−8594.
48. Claveau, D., and Riendeau, D. (2001) Mutations of the C-terminal end of cathepsin K affect proenzyme secretion and intracellular maturation, *Biochem. Biophys. Res. Commun. 281*, 551−557.
49. Wedemeyer, W. J., Welker, E., Narayan, M., and Scheraga, H. A. (2000) Disulfide bonds and protein folding, *Biochemistry 39*, 4207−4216.
50. Qiu, H., Edmunds, T., Baker-Malcolm, J., Karey, K. P., Estes, S., Schwarz, C., Hughes, H., and Van Patten, S. M. (2003) Activation of human acid sphingomyelinase through modification or deletion of C-terminal cysteine, *J. Biol. Chem. 278*, 32744−32752.
51. Wilbourn, B., Nesbeth, D. N., Wainwright, L. J., and Field, M. C. (1998) Proteasome and thiol involvement in quality control of glycosylphosphatidylinositol anchor addition, *Biochem. J. 332*, 111−118.
52. Liu, W. S., and Heckman, C. A. (1998) The sevenfold way of PKC regulation, *Cell. Signalling 110*, 529−542.
53. Insel, P. A., and Ostrom, R. S. (2003) Forskolin as a tool for examining adenylyl cyclase expression, regulation, and G protein signaling, *Cell. Mol. Neurobiol. 23*, 305−314.
54. Tesmer, J. J., and Sprang, S. R. (1998) The structure, catalytic mechanism and regulation of adenylyl cyclase, *Curr. Opin. Struct. Biol. 8*, 713−719.
55. Seibenhener, M. L., Babu, J. R., Geetha, T., Wong, H. C., Krishna, N. R., and Wooten, M. W. (2004) Sequestosome 1/p62 is a polyubiquitin chain binding protein involved in ubiquitin proteasome degradation, *Mol. Cell. Biol. 24*, 8055−8068.
56. Zeidan, Y. H., and Hannun, Y. A. (2007) Activation of acid sphingomyelinase by protein kinase Cδ-mediated phosphorylation, *J. Biol. Chem. 282*, 11549−11561.
57. Santana, P., Pena, L. A., Haimovitz-Friedman, A., Martin, S., Green, D., McLoughlin, M., Cordon-Cardo, C., Schuchman, E. H., Fuks, Z., and Kolesnick, R. (1996) Acid sphingomyelinase-deficient human lymphoblasts and mice are defective in radiation-induced apoptosis, *Cell 86*, 189−199.
58. Ogretmen, B., and Hannun, Y. A. (2004) Biologically active sphingolipids in cancer pathogenesis and treatment, *Nat. Rev. Cancer 4*, 604−616.

BI700817G